Targeting unknown and unstable periodic orbits

B. Doyon and L. J. Dubé
Département de Physique, de Génie Physique, et d'Optique, Université Laval, Cité Universitaire, Québec, Canada G1K 7P4

(Received 21 May 2001; published 7 March 2002)

We present a method to target and subsequently control (if necessary) orbits of specified period but otherwise unknown stability and position. For complex systems where the dynamics is often mixed [e.g., coexistence of regular and chaotic regions in area-preserving (Hamiltonian) systems], this targeting algorithm offers a way to not only gently bring the system from the chaotic domain to an unstable periodic orbit (where control is applied), but also to access *stable* regions of phase space (where control is not necessary) from *within* the stochastic regions. The technique is quite general and applies equally well to dissipative or conservative discrete maps and continuous flows.

DOI: 10.1103/PhysRevE.65.037202 PACS number(s): 05.45.−a, 05.45.Gg

One measure of scientific and technological progress is perhaps our improving ability to control the outcome of various processes of interest. This is especially true when one considers a complex system [1], the dynamics of which is rich, diverse, and often of ''constrained'' stochasticity. Since the theoretical [2] and experimental [3] demonstration of the possibility of control of deterministic chaos, we have witnessed a wealth of applications and improvements and alternatives over the initial approach of Ott, Grebogi, and Yorke (OGY) [2] that have been proposed and implemented ([4] and references therein).

The main feature of most control algorithms is to apply *small* and carefully chosen perturbations to an accessible system's parameter in order to maintain its motion in one of its many unstable states. For the perturbations to be small, they are usually applied if the system enters a small neighborhood of the unstable state of interest. One then relies on the ergodicity of the chaotic motion to guarantee that the system will eventually visit a region close to the unstable state. Quite often though, the waiting time can be too long for the control to take place and targeting strategies [5,6] are needed to steer the trajectory to the desired region.

The task of *standard* targeting algorithms is to construct a (possibly optimal) path that joins an initial state I to a preassigned target state T. In order to reach T, one pieces together local information that is successively used to construct a routing network to the final destination. Therefore local and global knowledge of phase space must be known or acquired to complete the procedure. In contrast, we propose a simple, general, and efficient algorithm to target and control states of chaotic systems with the more modest goal of reducing the complexity of the dynamics by bringing the system to one of its periodic orbits for a specific period m. Nothing is further assumed, however, about the position and stability of the final target (i.e., one ignores *a priori* which of the many possible period-m states will actually be reached and stabilized).

Let us consider that the state $\mathbf{x}_n$ of a system is represented by a D-dimensional nonlinear map

$$\mathbf{x}_{n+1}=\mathbf{F}(\mathbf{x}_n,p), \tag{1}$$

where $\mathbf{F}$ is either given explicitly, obtained numerically (e.g., by integration of a differential equation), or reconstructed from an experimental signal by standard embedding techniques [7,8]. We plan local interventions through programmed alterations of an accessible system's parameter p around a nominal value p_0. The system is supposed chaotic for $p\sim p_0$ with a chaotic regime offering an unlimited (large) number of unstable periodic orbits (UPOs). In order to intervene, we must provide intermediate links, i.e., *local targets*, which may be part of a trajectory leading to a period-m orbit.

We achieve this by using a recently proposed method of Schmelcher and Diakonos [9] that efficiently detects periodic orbits in chaotic systems. The key of the method is the application to the original system of a universal linear transformation that modifies the stability of the UPOs without altering their positions in phase space. We will refer to the technique as the stability transform algorithm (STA). Although first derived and exploited for dissipative maps, it is also applicable to area-preserving mappings [10] and can easily be extended to flows [11]. For our purpose, the decisive property of the method is its *global* character. Indeed, in the phase space of the original system, all initial states are made to converge to a component of a periodic orbit or to diverge to infinity. The basins of attraction of the sets of periodic orbits (of a given period) are large and cover a sizeable portion of phase space when compared to the neighborhood used in standard control strategies. The particular transformation (for the search for period-m orbits) is given by

$$\mathbf{y}_{i+1}=\mathbf{y}_i+\lambda\mathbf{C}[\mathbf{F}^{(m)}(\mathbf{y}_i,p_0)-\mathbf{y}_i], \tag{2}$$

where $\mathbf{y}$ denotes the state of the transformed system, $0<\lambda\ll 1$ is an adjustable constant, $\mathbf{F}^{(m)}(\mathbf{y},p)$ stands for the m times iterated map, and $\mathbf{C}$ is an orthogonal $D\times D$ matrix with element $C_{ij}\in\{0,\pm 1\}$ and whose rows and columns contain only one entry different from zero (see [9] for further details). Our algorithm reads therefore like this.

First, since an STA orbit will eventually bring the transformed system to a component of a periodic orbit, we will adjust the control parameter p such that, for a period-m orbit, the next iterate $\mathbf{x}_{n+m}$ falls on (or near) the position of a *local target* defined by $\overline{\mathbf{x}}=\mathbf{x}_n+\lambda\mathbf{C}[\mathbf{F}^{(m)}(\mathbf{x}_n,p_0)-\mathbf{x}_n]$ as prescribed by one STA step. In essence, we attempt to attach the chaotic orbit to a nearby STA trajectory by changing p_0 to $p_n = p_0 + \delta p_n$.

Second, to obtain an explicit expression for δp_n, we impose the *control criterion* that $\|\overline{\mathbf{x}} - \mathbf{x}_{n+m}(p_n)\|$ should be minimum. For $|\delta p_n| \ll 1$, the linearization

$$\mathbf{x}_{n+m}(p_n) = \mathbf{F}^{(m)}(\mathbf{x}_n, p_n) \sim \mathbf{F}^{(m)}(\mathbf{x}_n, p_0) + \mathbf{V}_n \delta p_n, \quad (3)$$

where $\mathbf{V}_n$ expresses the parametric variation of the map at $\mathbf{x}_n$, i.e., $\mathbf{V}_n = D_p \mathbf{F}^{(m)}(\mathbf{x}_n, p_0)$, together with the control criterion, gives

$$||\overline{\mathbf{x}} - \mathbf{x}_{n+m}|| \sim ||\mathbf{D}_n - \mathbf{V}_n \delta p_n|| = \text{minimum}. \quad (4)$$

Carrying out the minimization with $\mathbf{D}_n \equiv [\lambda \mathbf{C} - 1][\mathbf{F}^{(m)}(\mathbf{x}_n, p_0) - \mathbf{x}_n]$, one readily obtains

$$\delta p_n = \mathbf{D}_n \cdot \mathbf{V}_n / \|V_n\|^2. \quad (5)$$

Third and finally, if this calculated perturbation is smaller than our maximum tolerable range $|\delta p_n| \leq \delta p_{max} \ll |p_0|$, the perturbed system evolves according to $\mathbf{x}_{n+m} = \mathbf{F}^{(m)}(\mathbf{x}_n, p_n)$ otherwise it continues freely with $p_n = p_0$.

A number of points are worth mentioning. For one-dimensional (1D) systems, as soon as a small neighborhood of a periodic point is reached, the control step is identical to the occasional proportional feedback [12] for a specific value of λ. For higher dimensions, as expected also, once the targeting has been successful to bring the trajectory close to a UPO, Eq. (5) becomes similar to the minimal expected deviation method introduced in [13] for $\lambda = 0$. For flows, the map $\mathbf{F}^{(m)}$ is obtained by sampling the continuous trajectory on a Poincaré section at every m piercing. Furthermore, if a *learning phase*, i.e., a sufficiently long preregistered time series, is available, one can also use the information gained to approximate $\mathbf{F}^{(m)}$ and $\mathbf{V}_n$. Experience shows that our targeting algorithm remains robust under these conditions. Moreover, if the time series is used to map out beforehand the basins of attraction of certain specific UPOs, the targeting algorithm can be turned into a *directed* targeting and control procedure to well-defined targets. One further attractive feature of this method is that besides its ability to target a periodic orbit from afar, the STA step can bring the system to an unstable *or* a stable periodic orbit, since the stability of the latter is unchanged under the transformation. For Hamiltonian systems with mixed dynamics [14], we can therefore expect to access regions of regularity from within the stochastic sea. Concurrently, the method offers the possibility to cross Kolmogorov-Arnold-Moser (KAM) tori and accelerate transport to distant regions of phase space.

To illustrate the flexibility and some of the capabilities of the algorithm, we have chosen three 2D examples of increasing complexity: a dissipative map, an area-preserving mapping, and an Hamiltonian flow.

The first system under study is the Hénon map

$$x_{n+1} = 1 + y_n - A x^2, \quad y_{n+1} = B x_n.$$

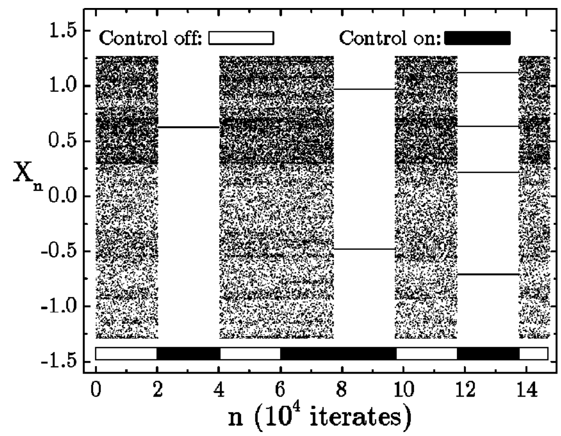

FIG. 1. Targeting and control scenario for the Hénon map ($A_0 = 1.4$ and $B_0 = 0.3$). Period-1, -2, and -4 orbits are successively targeted and held under control for 2×10^4 iterations.

The regime investigated is for nominal values $A_0 = 1.4$ and $B_0 = 0.3$. We use the parameter A for control and set $\delta p_{max} = 0.005 A_0$. To simulate an experimental context, we suppose that we do not know the application explicitly but rather estimate $\mathbf{F}(\mathbf{x}_n, p)$ to apply Eq. (5) with a simple nonlinear predictor (the Lorenz method of analogs [15]) applied to a previously recorded data set. The same predictor is also used to obtain $\mathbf{V}_n$ from a second recorded data set created for $p = p_0 + \Delta p$ $(\Delta p \ll p_0)$. Despite its simplicity, the predictor allows the targeting procedure to perform quite well. The results of a particular scenario are shown on Fig. 1. The control is held, in turn, for 2×10^4 iterates of period-1, -2, and -4 orbits. Once a UPO is controlled for the required number of iterates, control is released and δp_n is set to 0 for 2×10^4 iterates before the next control attempt. One observes that for period 2, the transient time to control is quite large ($\sim 2 \times 10^4$ iterates). The small value of δp_{max} [(1/2)% of the parameter A_0] was actually chosen to display a long transient interval. For larger values of δp_{max}, say ten times larger, the waiting times are essentially instantaneous on the scale of Fig. 1.

Our next example describes conservative billiard dynamics [16], consisting of a particle moving on a plane bounded by a closed curve. It serves to illustrate the transition from strict regularity (integrability) to chaos (ergodicity) in Hamiltonian system [17] and bears important connections to *quantum chaos* as well [18]. Besides its fundamental interest, this system has important physical relevance in that it adequately simulates the behavior of a photon trap in microcavities [19] and helps understand the emission patterns of microlasers [20] in the so-called whispering-gallery and bowtie modes [21]. With this application in mind, we have chosen to study the 2D *oval billiard*;

$$r(\varphi) = 1 + e \cos 2\varphi,$$

which approximates well the shape of some microcavity lasers. Geometrically, the parameter e is a measure of the asymmetry of the surface with respect to circularity, and dynamically, it is a measure of nonintegrability since $e = 0$ rep-

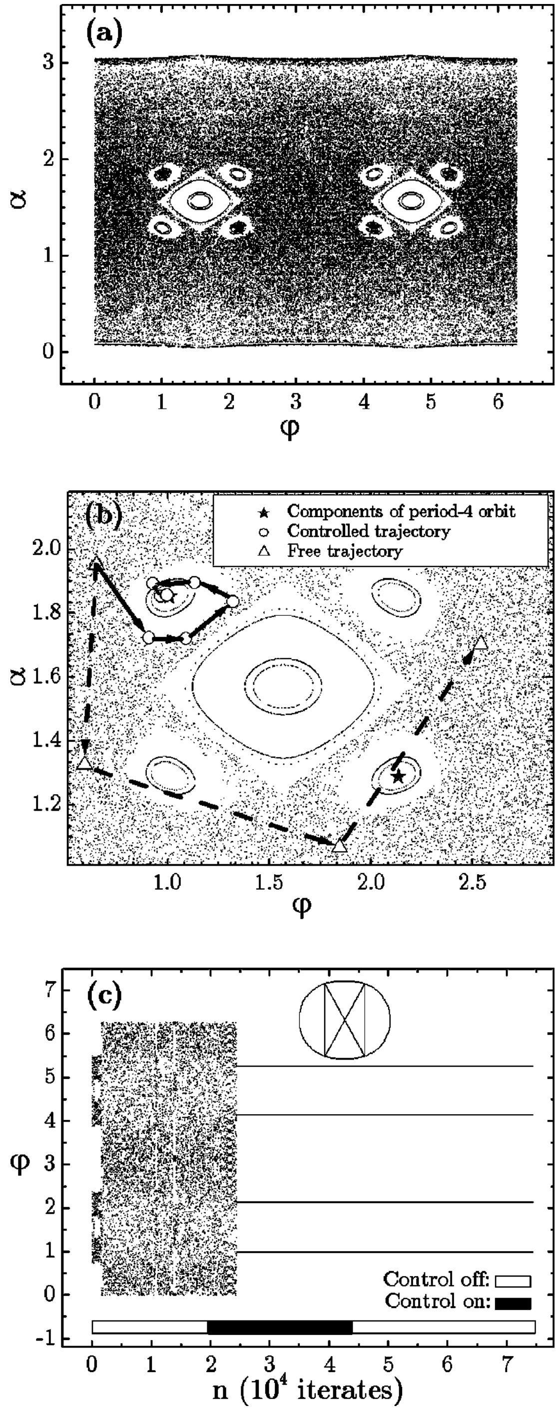

FIG. 2. (a) Phase space for the oval billiard ($e_0 = 0.15$). A (stable) period-4 orbit is indicated by stars; (b) enlarged section of phase space showing the path followed by the free and the controlled trajectories; (c) targeting and control scenario where the stable bowtie mode is reached from within the chaotic sea. The motion remains periodic after the control is turned off.

resents the integrable limit. For all $e \neq 0$, there are finite regions of phase space that contain chaotic trajectories. In Fig. 2(a), we show the mixed and complex structure of phase space for $e_0 = 0.15$: the state variables are the incident angles on the surface, $\{\alpha_n\}$, and the polar angles of the point of impact, $\{\phi_n\}$. The position of a stable period-4 orbit is indicated by a star and lies in a region of regularity. We apply the programmed perturbation on e ($\delta p_{max} = 0.05 e_0$) for a trajectory initially in the chaotic region and set the algorithm for the targeting of period 4. Figure 2(b) is an enlarged capsule where one shows the path taken by a few iterates of a free trajectory versus the controlled trajectory. It is clear that the controlled orbit has been captured by the STA trajectory leading to the stable period-4 orbit lying within a regular island. A usual control strategy would have been oblivious to the presence of that stable island. Furthermore, the attachment takes place at a distance of order one whereas usual control techniques impose a control neighborhood of at least two orders of magnitude smaller to keep the perturbations small. The targeting and subsequent stabilization is displayed in Fig. 2(c). Once control is released, the particle stays on the stable orbit that corresponds here to a bowtie-shaped orbit (inset). In this simulation, the targeting procedure has allowed a transition from an unstable whispering-gallery orbit [an initial condition around the upper part of Fig. 2(a)] to a stable bow-tie trajectory. In the context of microcavity lasers, this means a transition from a nondirectional low-power laser to a highly directional high-power one [21]. This may potentially be quite useful, and possible experimental implementations of this technique are being examined.

Our final example is a continuous, two degrees of freedom (4D phase space) Hamiltonian system. It represents the motion of an electron under the combined influence of a Coulomb and a magnetic field. It goes under the name *diamagnetic Kepler problem* and just as the previous system, it occupies central stage in classical and quantum chaos research [18]. It has proven useful [22] to consider a (pseudo-) Hamiltonian function in scaled semiparabolic coordinates (here for angular momentum $L = 0$),

$$\hat{h} = \frac{1}{2}(p_\mu^2 + p_\nu^2) - \epsilon(\mu^2 + \nu^2) + \frac{1}{8}\mu^2\nu^2(\mu^2 + \nu^2) \equiv 2$$

for the dynamical evolution, where ϵ acts as a dynamical parameter and is related to the physical energy E by $\epsilon = \gamma^{-2/3} E$. The parameter $\gamma = B/B_c$ denotes the strength of the magnetic field relative to the unit $B_c \simeq 2.35 \times 10^5$ T. As ϵ is varied, the classical flow of $\hat{h}$ covers a wide range of Hamiltonian dynamics reaching from bound, nearly integrable behavior to completely chaotic and unbound motion [22]. Control of this chaotic motion by a fully numerical OGY technique has been recently reported [11].

The dimension reduction (from 4D to 2D) and the discretization to obtain $\mathbf{F}^{(m)}(\mathbf{x}, p)$ is performed by observing the dynamics on the Poincaré section defined by $\mu = 0$, $\dot{\mu} > 0$. For the target and control scenario, we use parameter ϵ with nominal value $\epsilon_0 = -0.2$ ($\delta p_{max} = 0.05 |\epsilon_0|$). We ask the targeting and control of two different orbits: period-2 and period-3 orbits, both for 2×10^4 iterates and turn the control off for the first 2×10^4 iterates before each attempt. Results are shown in Fig. 3. The first controlled period is in the chaotic band. When control is released, the motion returns to the chaotic regime. The period-3 orbit, however, lies in a

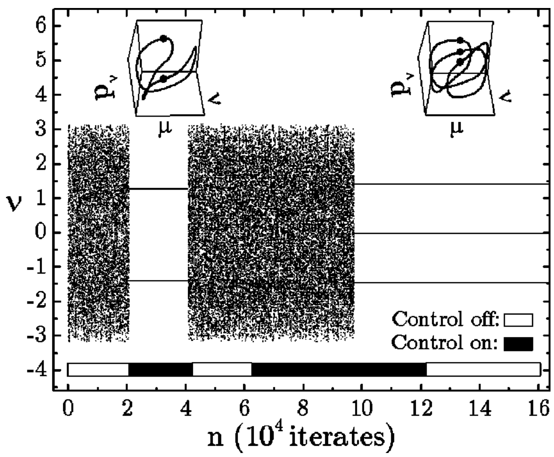

FIG. 3. Targeting and control scenario for the diamagnetic Kepler problem ($\epsilon_0 = -0.2$). The period-2 orbit reached is unstable whereas the period-3 orbit is stable.

regular island. Once the system is brought to this stable orbit, control can be released and the motion stays regular. The corresponding 3D trajectories are shown in the insets. One notices that the waiting time to stabilize the period-3 orbit appears quite long ($\sim 4 \times 10^4$ iterates). The reason for this is interesting. The stable orbit lies in the middle of a tiny regular island (5×10^{-3} across) outside of which an *unstable* period-3 orbit is located. This proximity of two period-3 orbits produces intricate basins of attraction for the STA step and a corresponding longer time to ''decide'' between the possible targets. This situation is, however, atypical.

We have presented a targeting and control algorithm that combines the strength of a global periodic orbit seeking procedure with a control minimization that directs a chaotic system to an orderly state. The method is quite general as it applies to discrete and continuous time evolution of dissipative or conservative character. Its ability to operate with modest information and to reach *stable* states of systems displaying mixed dynamics stands out as an important feature not easily available in other targeting strategies. As the interest for complex systems continues to grow, our method offers a possibility for the reduction of their dynamical complexity, whether it be for physical, engineering or therapeutic purposes. Details of our approach (efficiency, robustness to noise, etc.) are being prepared for publication together with its extension to a wider class of systems (e.g., reversible systems [23] where conservative *and* dissipative behaviors coexist).

We acknowledge financial support by FCAR (Québec) and NSERC (Canada). The authors are grateful to Carl Robert for a careful reading of the manuscript.

[1] R. Badii and A. Politi, *Complexity, Hierarchical Structures and Scaling in Physics* (Cambridge University Press, Cambridge, 1999).

[2] E. Ott, C. Grebogi, and J.A. Yorke, Phys. Rev. Lett. **64**, 1196 (1990).

[3] W.L. Ditto, S.N. Rauseo, and M.L. Spano, Phys. Rev. Lett. **65**, 3211 (1990).

[4] S. Boccaletti, C. Grebogi, Y.-C. Lai, H. Mancini, and D. Maza, Phys. Rep. **329**, 103 (2000).

[5] T. Shinbrot *et al.*, Phys. Rev. Lett. **65**, 3215 (1990); E.J. Kostelich *et al.*, Phys. Rev. E **47**, 305 (1993); E. Barreto *et al.*, *ibid.* **51**, 4169 (1995); Y.C. Lai, Phys. Lett. A **221**, 376 (1996).

[6] E.M. Bollt and J.D. Meiss, Physica D **81**, 280 (1995); C.G. Schroer and E. Ott, Chaos **7**, 512 (1997).

[7] F. Takens, in *Dynamical Systems and Turbulence*, edited by D.A. Rand and L.S. Young, Lecture Notes in Mathematics Vol. 898 (Springer-Verlag, New York, 1981).

[8] T. Sauer, J. Yorke, and M. Casdagli, J. Stat. Phys. **65**, 579 (1991).

[9] P. Schmelcher and F.K. Diakonos, Phys. Rev. Lett. **78**, 4733 (1997); Phys. Rev. E **57**, 2739 (1998); F.K. Diakonos, P. Schmelcher, and O. Biham, Phys. Rev. Lett. **81**, 4349 (1998).

[10] B. Pourbohloul, Ph.D. thesis, Université Laval, 1999.

[11] B. Pourbohloul and L.J. Dubé, e-print nlin-sys/0008001; L.J. Dubé and P. Després, in *The Physics of Electronic and Atomic Collisions*, edited by Yukikazu Itikawan *et al.*, AIP Conf. Proc. 500 (AIP, Melville, NY, 2000), p. 551; B. Pourbohloul, B. Doyon, and L.J. Dubé (unpublished).

[12] E.R. Hunt, Phys. Rev. Lett. **67**, 1953 (1991).

[13] C. Reyl, L. Flepp, R. Badii, and E. Brun, Phys. Rev. E **47**, 267 (1993).

[14] R.S. MacKay and J.D. Meiss, *Hamiltonian Dynamical Systems* (Adam Hilger, Bristol, 1987).

[15] E.N. Lorenz, J. Atmos. Sci. **26**, 636 (1969).

[16] G.D. Birkhoff, Acta Math. **50**, 359 (1927).

[17] M.V. Berry, Eur. J. Phys. **2**, 91 (1981); M. Robnik, J. Phys. A **16**, 3971 (1983).

[18] R. Blümel and W.P. Reinhardt, *Chaos in Atomic Physics* (Cambridge University Press, Cambridge, 1997).

[19] S.L. McCall, A.F.J. Levi, R.E. Slusher, S.J. Pearton, and R.A. Logan, Appl. Phys. Lett. **60**, 289 (1992).

[20] J.U. Nöckel and A.D. Stone, Nature (London) **385**, 45 (1997).

[21] C. Gmachl, F. Capasso, E.E. Narimanov, J.U. Nöckel, A.D. Stone, J. Faist, D.L. Sivco, and A.Y. Cho, Science **280**, 1556 (1998).

[22] J.B. Delos, S.K. Knudson, and D.W. Noid, Phys. Rev. A **30**, 1208 (1984); H. Friedrich and D. Wintgen, Phys. Rep. **183**, 37 (1989).

[23] J.A.G. Roberts and G.R.W. Quispel, Phys. Rep. **216**, 63 (1992).